ISSN 0454－4641

運輸省港湾技術研究所

港湾技術研究所報告

REPORT OF THE PORT AND HARBOUR RESEARCH INSTITUTE

MINISTRY OF TRANSPORT

VOL. 36 NO. 2 JUNE. 1997

NAGASE, YOKOSUKA, JAPAN

港湾技術研究所報告（REPORT OF P.H.R.I.）

第36巻　第2号（Vol.36,No.2），1997年6月（June. 1997）

目　　次（CONTENTS）

港湾技術研究所報告
第36巻第2号(1997.6)

兵庫県南部地震におけるニューマチックケーソン式の橋梁基礎の変形に関する有効応力解析

Hanlong LIU*
井合 進**
一井康二***
森田年一***
岡下勝彦****

要旨

1995年1月17日の兵庫県南部地震において，神戸港の多数の港湾施設及び臨港施設が被災した。神戸大橋のニューマチックケーソン基礎の被災もその一つである．神戸大橋のニューマチックケーソン基礎は約30mの根入れを持つにもかかわらず，ケーソン上面で約0.6mから0.8mの海側への残留変形を生じた．本研究は，そのニューマチックケーソン基礎の被災メカニズムについて，土－構造物の相互作用を考慮できるような2次元有効応力解析によって検討を加えたものである．解析モデルとしては，主応力軸の回転を自然に考慮できるところに特徴がある，ひずみ空間における多重機構に基づくモデルを用いた．基盤における入力地震動としてはポートアイランドGL－83mで神戸市開発局によって観測された波形を用いた．解析の結果，ケーソンの天端で0.46m及び0.48mの海側への水平変位が得られ，上述の実被害とオーダー的に整合する結果が得られた．また，検討の結果，基礎部分における過剰間隙水圧の上昇により，岸壁の変形量は大きく影響されていることがわかった．あわせて，基礎周辺における地盤改良の効果についても検討を加えた．

キーワード：有効応力解析，残留変形，液状化，ニューマチックケーソン基礎

＊ 構造部地盤震動研究室客員研究員
＊＊ 構造部地盤震動研究室室長
＊＊＊ 構造部地盤震動研究室
＊＊＊＊神戸市港湾局

REPORT OF THE PORT AND
HARBOUR RESEARCH INSTITUTE
Vol. 36, No. 2 (June. 1997)

EVALUATION OF DEFORMATION TO THE PNEUMATIC CAISSON FOUNDATIONS OF THE KOBE OHASHI BRIDGE

HANLONG LIU*
SUSUMU IAI**
KOJI ICHII***
TOSHIKAZU MORITA***
KATSUHIKO OKASHITA****

Synopsis

Many earth structures and foundations were damaged in Kobe port area during the 1995 Great Hanshin earthquake. Damage to the pneumatic caisson foundations for the Kobe Ohashi bridge was of a particular interest. Though the pneumatic caissons were embedded to a depth of K.P.-31m, there were about 0.6 to 0.8m seaward displacement induced at the caissons. In order to identify the mechanism of deformation, a two-dimensional effective stress analysis is performed to take into account the soil-structural and water-structural interactions in this study. The constitutive model used is a multiple shear mechanism type defined in strain space and can take into account the effect of rotation of principal stress axis directions. The earthquake acceleration recorded at a depth of 83 meters on the Port Island during the 1995 Great Hanshin earthquake is used as input bedrock motion. The results of analysis show that the seaward residual displacements are 0.46 m at the top of a caisson and 0.48 m at the top of the other caisson, resulting in a total of 0.94m. The order of computed residual displacement is in good agreement with the measured. The results indicate that the excess pore water pressure increase in the foundation significantly affected the performance of caissons. The effect of soil improvement is also discussed.

Key words : Kobe Ohashi bridge, pneumatic caisson foundation, effective stress analysis, liquefaction, residual deformation

* Guest researcher, Geotechnical Earthquake Engineering Laboratory, Port and Harbour Research Institute. On leave of Geotechnical Engineering Research Institute, Hohai University, Nanjing, 210098, China

** Chief, Geotechnical Earthquake Engineering Laboratory, Port and Harbour Research Institute, Ministry of Transport, 3-1-1, Nagase, 239, Japan

*** Geotechnical Earthquake Engineering Laboratory, Port and Harbour Research Institute, Ministry of Transport, 3-1-1, Nagase, 239, Japan

**** Port Bureau, Kobe City

CONTENTS

1. INTRODUCTION

Kobe port is located in the south of Kobe city about 17 km from the epicenter of the 1995 Great Hanshin earthquake. The Kobe Ohashi Bridge, 319 meters long, with a central span 217 meter long and two-side spans 51 meter long, lies on the site between the Fourth Pier and the Port Island in Kobe port area. It is the only bridge connecting the Port Island with the central area of Kobe city. There are two pneumatic concrete caissons P2 and P3 used for the foundations to support the main span of the bridge. Overall view of the Kobe Ohashi Bridge after the earthquake is shown in Photo 1, and the location and cross section are shown in **Fig. 1**. As shown in this figure, the shoe at the Port Island side(P3) is fixed whereas the one at the Fourth Pier side(P2) is movable type.

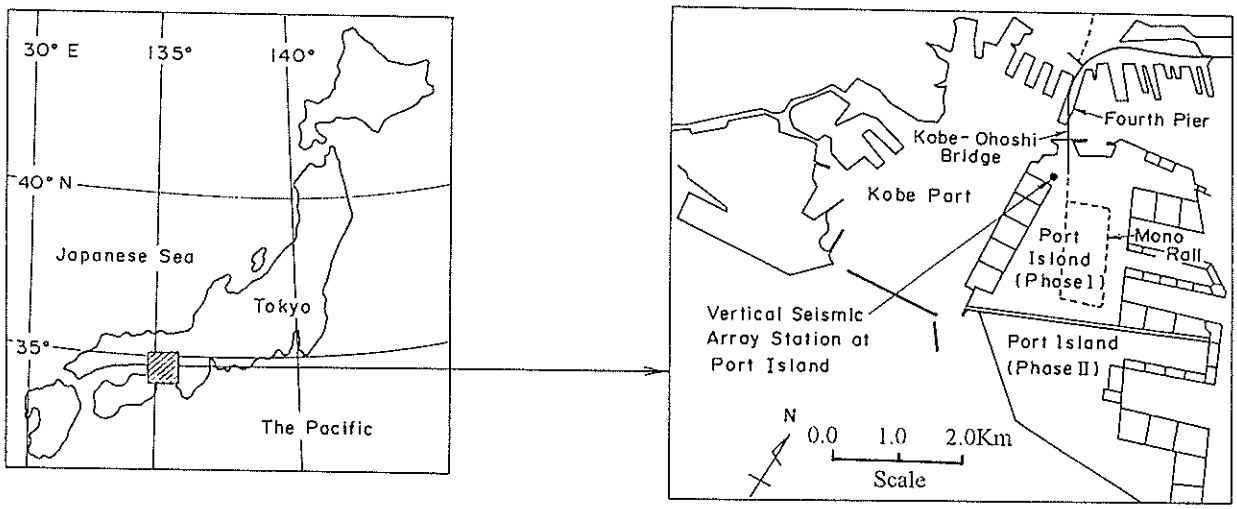

(a) Location

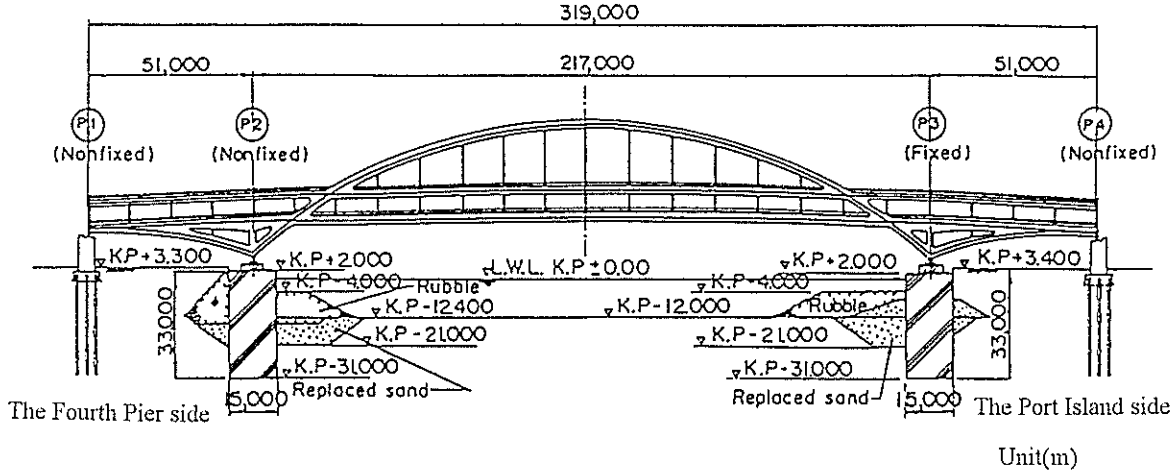

(b) Cross section

Fig. 1 The location and cross section of Kobe Ohashi Bridge

During the 1995 Great Hanshin earthquake, the bridge was shaken by a strong earthquake motion having the peak acceleration of 670 Gal and 172 Gal in the horizontal direction and vertical directions at the bedrock 83 meter deep from the ground surface. Though the pneumatic caissons were embedded in soil to a depth of K.P.-31m and founded on a firm foundation of Pleistocene origin, there were about 0.60 to 0.80m residual displacements toward sea and 0.36 to 0.93 degrees of seaward inclination after the earthquake. The relative residual displacement between the upper structure of bridge and the foundation at the Fourth Pier side(P2) is shown in **Photo. 2.** In order to identify the mechanism of the deformation for the foundation, an effective stress analysis was performed in this study using the results of the geotechnical investigations and in-situ velocity measurements.

Photo 1 Overview of the Kobe Ohashi Bridge

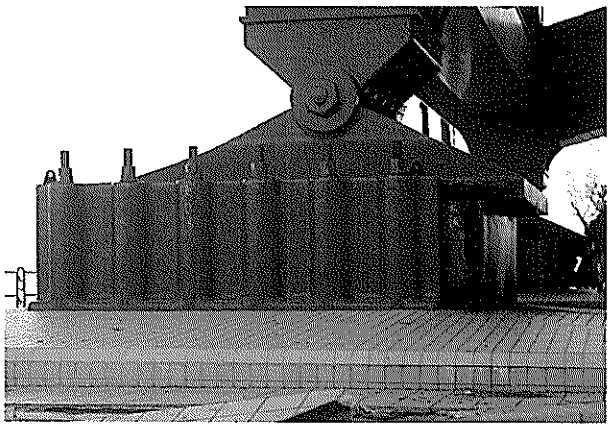

Photo 2 Residual displacement at the foundation P2

2. EFFECTIVE STRESS ANALYSIS

2.1 Constitutive Equations

The constitutive model used in this study is a strain space plasticity type and consists of a multiple shear mechanism in the plane strain condition[1]. With the effective stress and strain vectors written by

$$\{\sigma'\}^T = \{\sigma'_x, \sigma'_y, \tau_{xy}\} \tag{1}$$

$$\{\varepsilon\}^T = \{\varepsilon_x, \varepsilon_y, \gamma_{xy}\} \tag{2}$$

the basic form of the constitutive relation is given by

$$\{d\sigma'\} = [D](\{d\varepsilon\} - \{d\varepsilon_p\}) \tag{3}$$

in which

$$[D] = K\{n^{(o)}\}\{n^{(o)}\}^T + \sum_{i=1}^{I} R_{L/U}^{(i)}\{n^{(i)}\}\{n^{(i)}\}^T \tag{4}$$

In this relation, the term $\{d\varepsilon_p\}$ in Eq.(3) represents the additional strain incremental vector to take the dilatancy into account and is given from the volumetric strain increment due to the dilatancy as

$$\{d\varepsilon_p\}^T = \{d\varepsilon_p/2,\ d\varepsilon_p/2,\ 0\} \tag{5}$$

The first term in Eq.(4) represents the volumetric mechanism with rebound modulus K and the direction vector is given by

$$\{n^{(o)}\}^T = \{1,\ 1,\ 0\} \tag{6}$$

The second term in Eq.(4) represents the multiple shear mechanism. Each mechanism $i = 1,2,\ldots,I$ represents a virtual simple shear mechanism, with each simple shear plane oriented at an angle $\theta_i/2+\pi/4$ relative to the x axis.

The tangential shear modulus $R_{L/U}^{(i)}$ represents the hyperbolic stress strain relationship with hysteresis characteristics. The direction vectors for the multiple shear mechanism in Eq.(4) are given by

$$\{n^{(i)}\}^T = \{\cos\theta_i, -\cos\theta_i, \sin\theta_i\} \quad (\text{for } i = 1,2,\ldots, I) \tag{7}$$

in which

$$\theta_i = (i-1)\Delta\theta \quad (\text{for } i = 1,2,\ldots, I) \tag{8}$$

$$\Delta\theta = \pi/I \tag{9}$$

A schematic figure for the multiple simple shear mechanism is shown in Fig. 2. Pairs of circles indicate mobilized virtual shear strain in positive and negative modes of compression shear(solid lines with darker hatching) and simple shear(broken lines with lighter hatching).

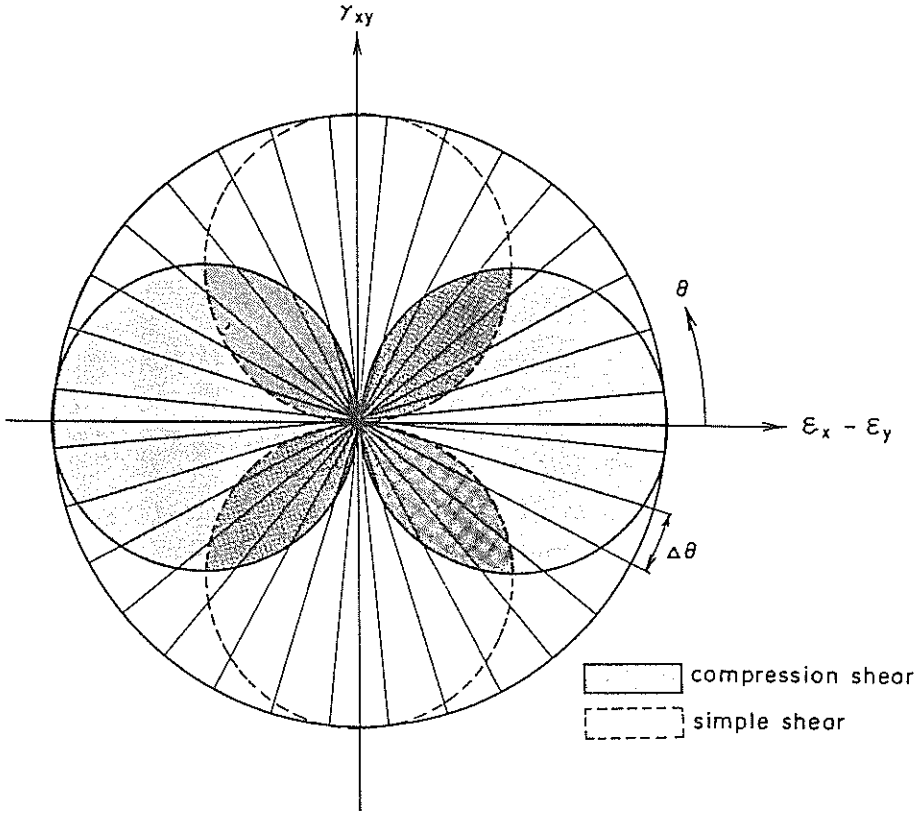

Fig. 2 Schematic figure for multiple simple shear mechanism

The loading and unloading for shear mechanism are separately defined for each virtual simple shear mechanism by the sign of $\{n^{(i)}\}^T\{d\varepsilon\}$. The multiple shear mechanism takes into account the effect of rotation of principal stress axis directions, the effect of which is known to play an important role in the cyclic behavior of anisotropically consolidated sand[2]. Ten parameters are needed for the present model; two of which characterize elastic properties of soil; another two specify plastic shear behavior, and the rest characterize dilatancy as shown in Table 1.

Table 1 Parameters of the present model

Parameters	Type of Mechanism	Kind of the parameters
K_a	Elastic volumetric	Rebound modulus
G_{ma}	Elastic shear	Shear modulus
ϕ_f	Plastic shear	Shear resistance angle
ϕ_p	Plastic dilatancy	Phase transformation angle
H_m	Plastic shear	Hysteretic damping factor at large shear strain level
p_1	Plastic dilatancy	Initial phase of dilatancy
p_2	Plastic dilatancy	Final phase of dilatancy
w_1	Plastic dilatancy	Overall dilatancy
S_1	Plastic dilatancy	Ultimate limit of dilatancy
c_1	Plastic dilatancy	Threshold limit

2.2 Finite Element Modeling

The finite element mesh shown in **Fig. 3** was used for the analysis of Kobe Ohashi Bridge under plane strain condition. Total of 2660 nodal points and 4654 elements were used. Five types of elements were used in the analysis; those were linear elements for caisson, nonlinear elements for sand and clay, beam elements for the upper structure of bridge, liquid elements for water and joint elements for the boundaries between a soil and a structure. The sea water was modeled as incompressible fluid and was formulated as an added mass matrix based on the equilibrium and continuity of fluid at the solid-fluid interface[3].

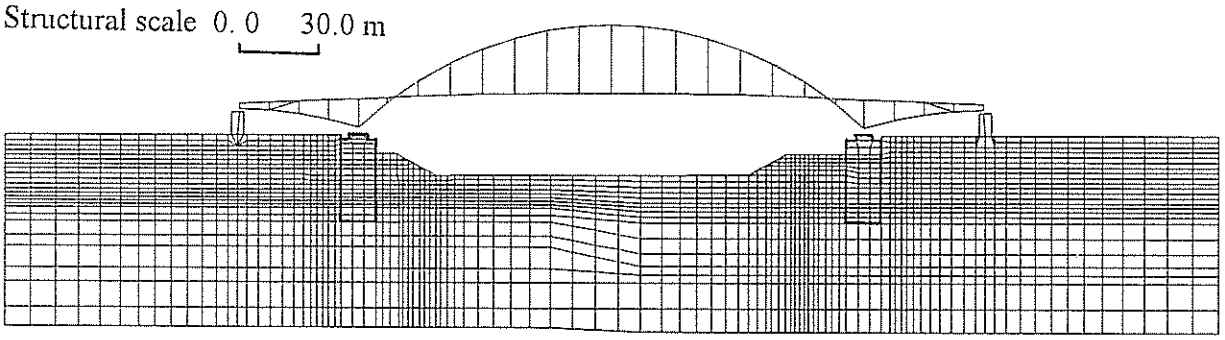

Fig. 3 Finite element mesh for Kobe Ohashi Bridge

Although the finite element analysis in this study was based on two dimensional analysis as mentioned earlier, actual configurations of the pneumatic caissons were three dimensional, having a horizontal rectangular cross section of 15 m by 15 m. The difference in two and three dimensional analyses may affect the results of the analysis in the following manner. If the main cause of the movement of the pneumatic caissons are due to the soil displacements around the caissons, then the two dimensional analysis will give conservative results (i.e. larger displacements) of the pneumatic caissons than the three dimensional analysis. This is because the two dimensional analysis does not allow the soil movement freely go through outside of the cross section of the pneumatic caissons. If, on the other hand, the main cause of the movement of the pneumatic caissons are due to the inertia force transmitted from the upper structure supported by the pneumatic caisson foundations, then the two dimensional analysis will give unconservative results (i.e. smaller displacements) than the three dimensional analysis. This is again because the two dimensional analysis does not allow the soil movement freely go through outside of the cross section of the pneumatic caissons, resulting in larger resistance from the foundation soil to the pneumatic caissons. As will be seen in the later chapter, the results by the analysis indicate the mechanism of deformation of the pneumatic caissons mainly due to the soil movement, pushing the pneumatic caissons towards sea. It is, thus, considered, that the assumption of the two dimensional analysis in this study resulted in conservative estimates of the movement of the pneumatic caissons (i.e. larger displacements).

2.3 Model Parameters

The model parameters were calibrated by referring to the in-situ velocity measurements and other relevant test results. Shown in **Fig. 4** were the results of the geotechnical investigations at the Fourth Pier and the Port Island in the vicinity of Kobe Ohashi Bridge.

The dilatancy parameters of fill soil and the sand replacing the original clay layer in Kobe Port were determined referring to Rokko Island data[4]. The dilatancy parameters for other soils were calibrated based on the SPT N-values and laboratory test results[5]. The calibrated liquefaction resistance curves are shown in **Fig. 5.** The computed effective stress path and stress strain relation for replaced sand are shown in **Fig. 6.** The calibrated parameters used

for the analysis are shown in **Table 2.** More details of the parameter calibration are shown in Appendix.

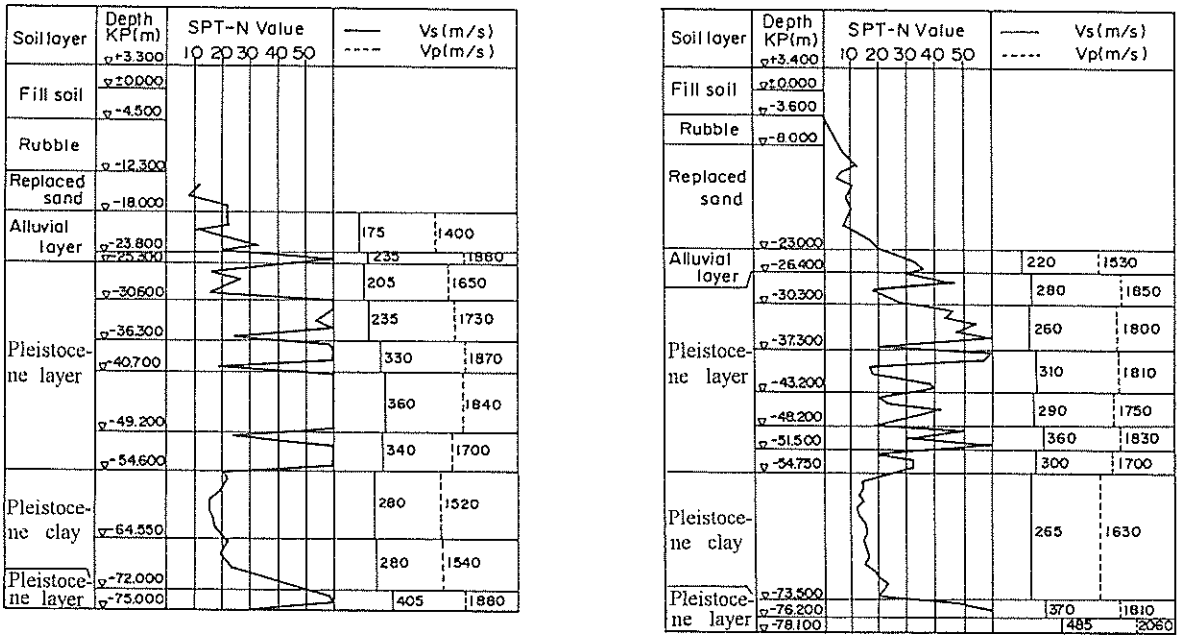

(a) The Fourth Pier (b) The Port Island

Fig. 4 In-situ investigation results

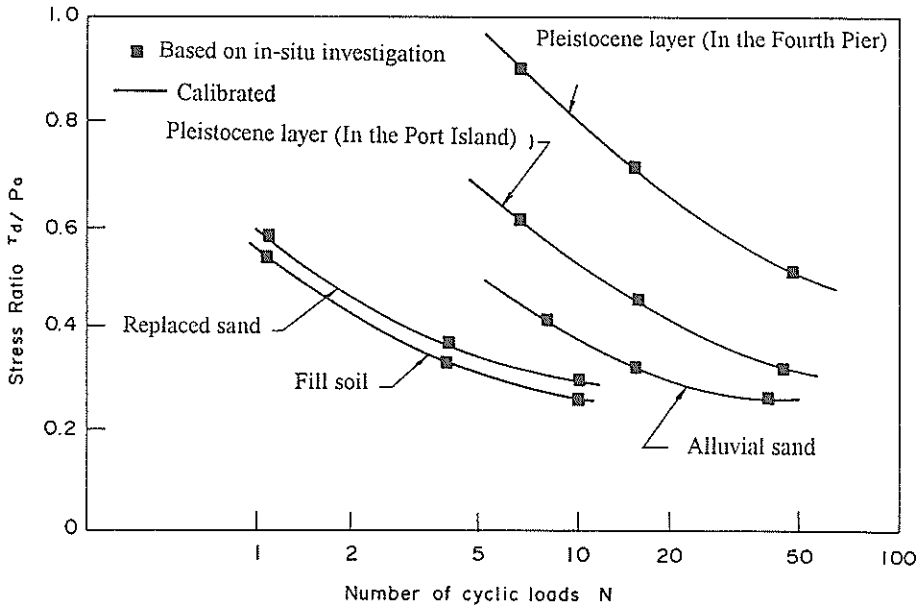

Fig. 5 Computed liquefaction resistance curve

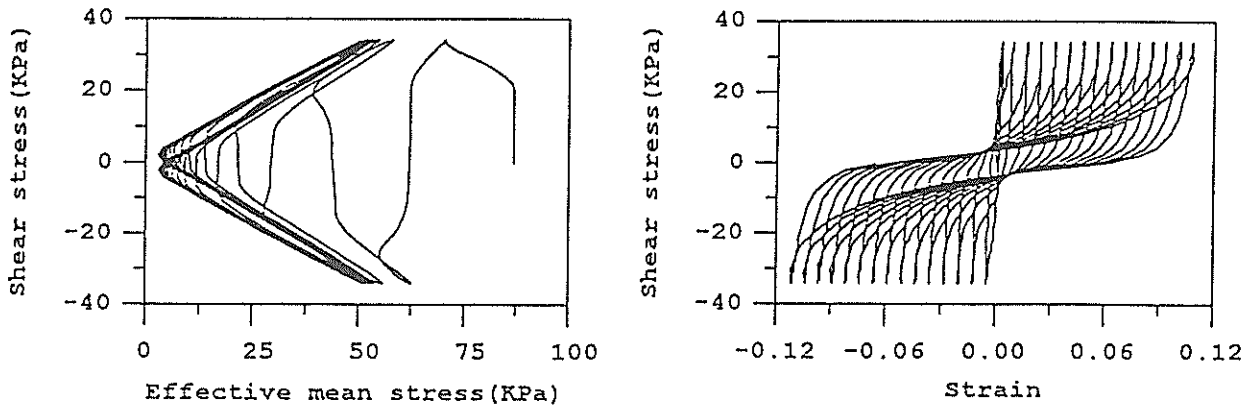

(a) Effective stress path (b) Stress vs. strain

Fig. 6 Computed cyclic behavior of replaced sand

Table 2 Model parameters used for the analysis

Layer No.	γ (tf/m^3)	G_a (tf/m^2)	K_{ma} (tf/m^2)	σ'_{ma} (tf/m^2)	ϕ_f (deg.)	ϕ_p (deg.)	Dilatancy parameters S_1	w_1	p_1	p_2	c_1
Fill soil	1.80	8000	20928	6.300	36	28	0.005	10.5	0.5	0.6	3.40
Replaced sand	1.80	7400	19358	10.60	36	28	0.005	5.50	0.6	0.8	2.30
Alluvial layer	1.96	6100	15958	14.67	36	28	0.005	16.0	0.5	0.8	2.50
Pleistocene layer(1)*	1.89	17000	44472	25.00	40	28	0.005	145.	0.5	0.6	25.3
Pleistocene layer(2)*	1.87	21000	54936	25.00	40	28	0.005	16.5	0.5	0.8	3.43
Replaced stone	1.92	18000	47088	22.27	40						
Clay layer	1.62	12000	31392	36.30	30						

* Pleistocene layer(1) is given for the Fourth Pier and Pleistocene layer(2) is given for the Port Island.

2.4 Input Accelerations

The earthquake motions were recorded with a vertical seismic array in the Port Island at the ground surface and at depths of 16 m, 32 m and 83m at the earthquake. The recording was successfully accomplished by the Kobe City.

The site of vertical seismic array was very close to the Kobe Ohashi Bridge with a distance of about 150m. The records at the depth of 83 m shown in **Fig. 7** was used as the bedrock motion in the effective stress analysis. The maximum horizontal acceleration is 670.6Gal in the N-S direction, while the maximum vertical acceleration is 172.4Gal. The direction component along the direction of Kobe Ohashi Bridge was the same as the N-S component of the recording, considering the orientation error of the seismograph[6].

Before the dynamic response analysis, a static analysis was performed to simulate the stress distributions to take the effect of gravity into account. The same constitutive model was used as in the earthquake response analysis but under drained condition. With these initial conditions and the parameters mentioned earlier, an earthquake response analysis was performed on the Kobe Ohashi Bridge. The analysis was conducted with the undrained conditions[7] in order to simplify the analysis. The numerical time integration was made based on Wilson-θ method (θ =1.4) using the time interval of 0.01 seconds. Rayleigh damping (α =0 and β =0.002) was used to ensure the stability of numerical solution process.

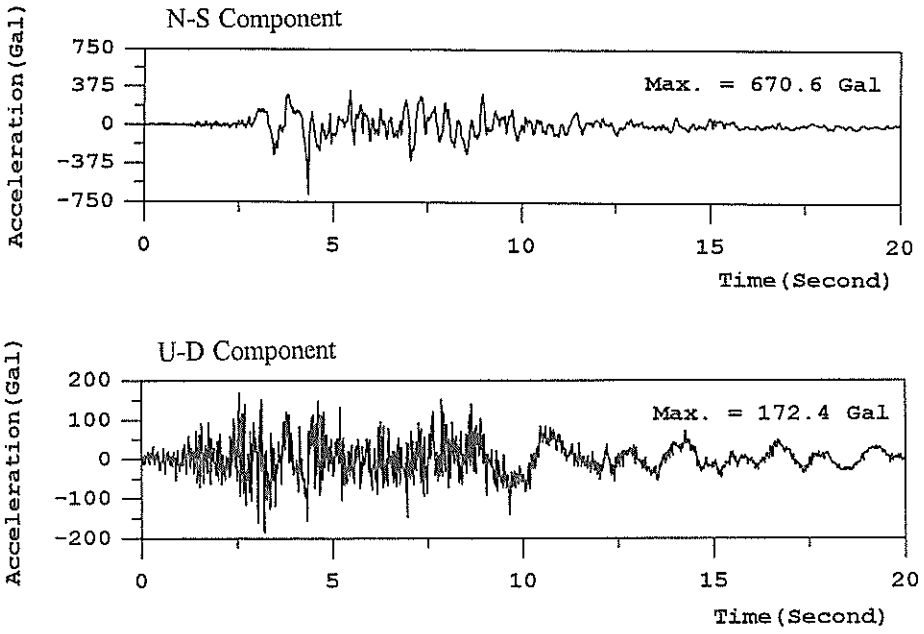

Fig. 7 Earthquake motion at 1995 Great Hanshin earthquake recorded at -83 meters on Port Island

3. RESULTS OF ANALYSIS

The results of the effective stress analysis of the Kobe Ohashi Bridge are shown in Figs. 8 and 9. Shown in Fig. 8 is the displacement and acceleration responses of Nodes 764 and 1658 at the top of caissons P2 and P3 indicated in Fig. 9(a). The displacements are gradually increased for about 15 seconds and then stayed close to the residual values. The deformed mesh shape and displacement vectors at the end of the earthquake are shown in Fig. 9(in the figure, the deformation is scaled five times as large for the plotting). The deformation in the foundation is mainly seen around the caissons and both of the caissons moved toward the sea. The computed and measured results for the caissons are summarized in Table 3. The computed horizontal displacements are 0.46 m at P2 and 0.48 m at P3, the settlement are 0.12m and 0.11m respectively, resulting in the total relative horizontal displacement of 0.94 m. The order of computed deformation was consistent well with the measured after earthquake.

Table 3 Measured and computed residual displacements

Items	Caisson	P2	P3
Horiz. disp	Computed(m)	0.46	0.48
	Measured(m)	Total:	0.60 - 0.80
Inclination	Computed(deg.)	0.68	0.07
	Measured(deg.)	0.36- 0.73	0.78 - 0.93

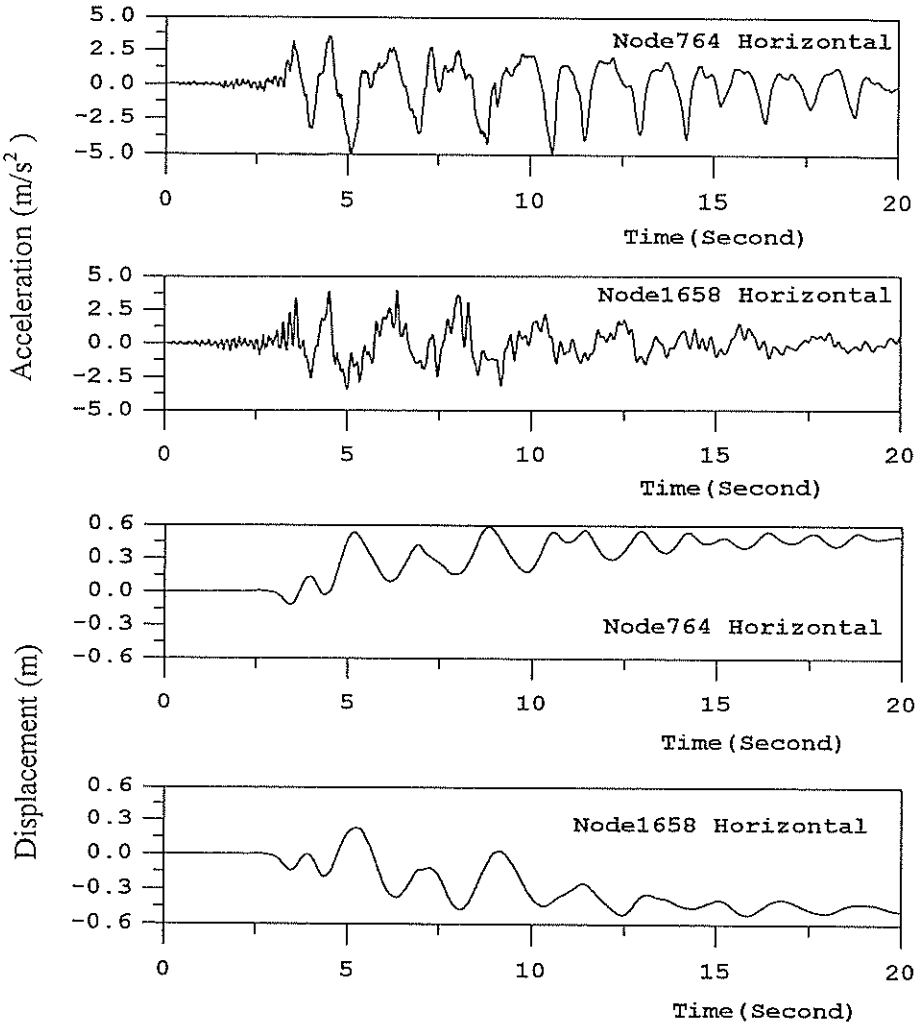

Fig. 8 Time history of deformation and acceleration

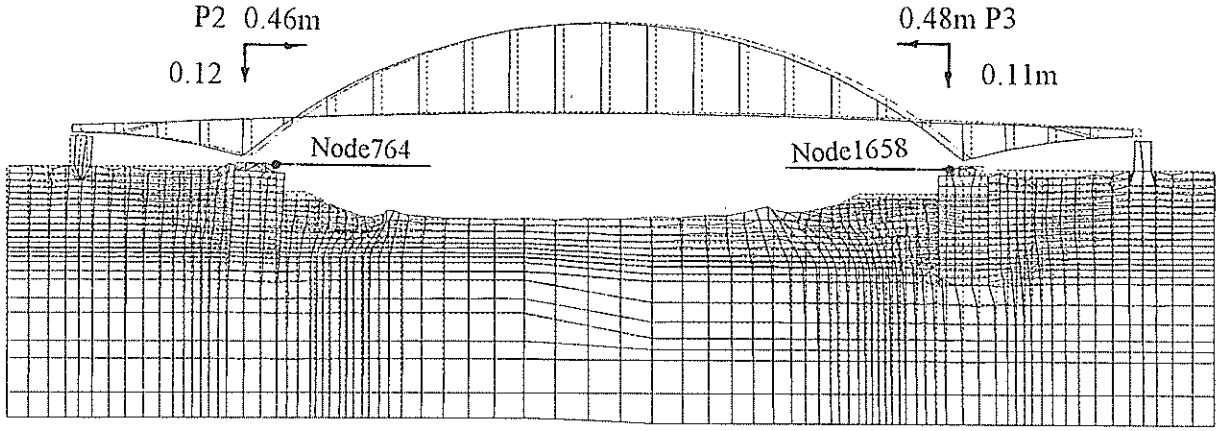

(a) The shape

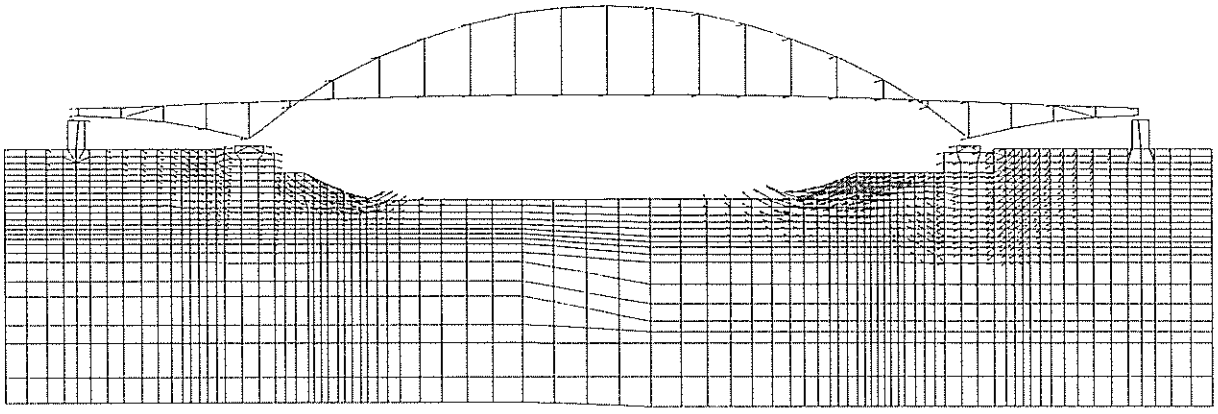

(b) The vector

Fig. 9 The shape and vectors of computed deformation(main part)

To evaluate the degree of liquefaction of the foundation, the excess pore water pressure ratio specified in terms of $(1-\sigma'_m/\sigma'_{m0})$ is computed, where σ'_m, σ'_{m0} are the current and initial mean effective stresses. The time histories of pore water pressure ratios of elements 384, 1819 in the fill soil and elements 710, 1463 in the replaced sand indicated in **Fig. 11** are shown in **Fig. 10.** The pore water pressures are gradually increased to the ratio of 0.85 for about seven seconds and then remain at these values until the end of earthquake. The residual displacements in **Fig.** 8 are increased with the increase of excess pore water pressure. Distribution of the computed excess pore water pressure ratio at the end of the earthquake is shown in **Fig. 11.** The high excess pore water pressures shown in **Fig.11** is speculated to have affected the performance of the pneumatic caissons for the Kobe Ohashi Bridge. This issue will be discussed in detail in Chapter 5.

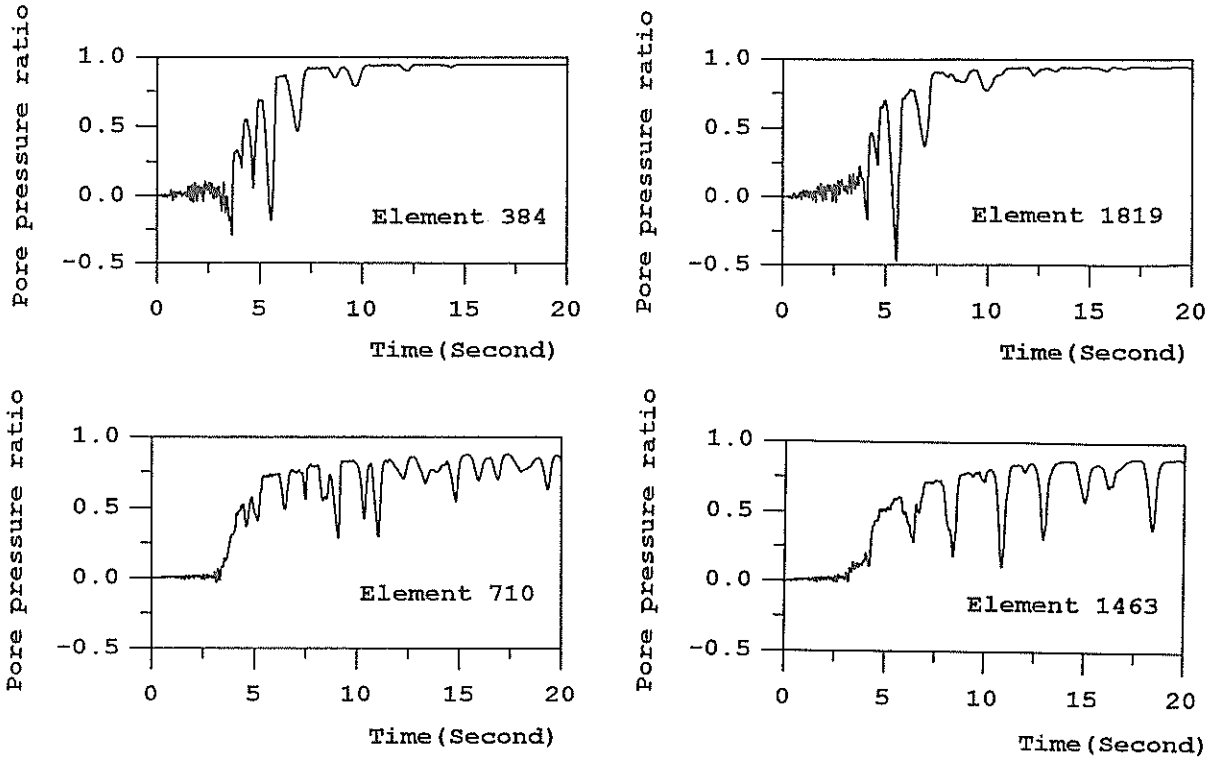

Fig. 10. Time history of excess pore water pressure ratio

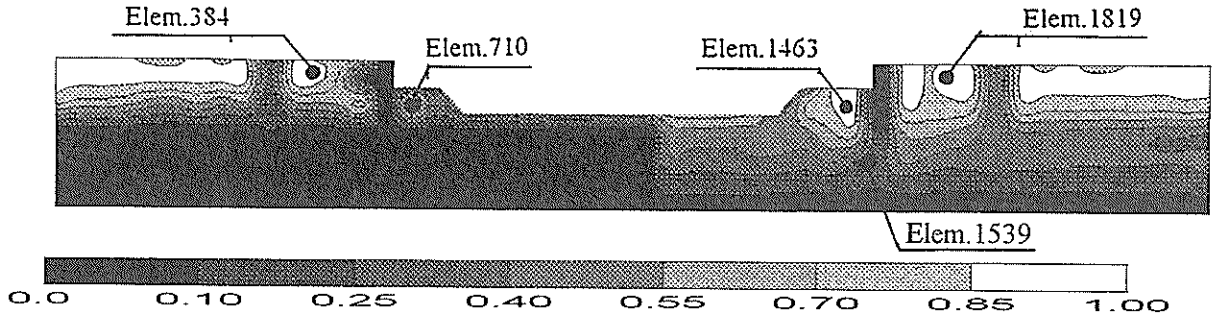

Fig. 11. The computed excess pore water pressure ratio

4. MECHANISM OF DEFORMATION

In order to look into the mechanism of deformation of pneumatic caisson foundations, the stress and strain of soils in the upper fill soil and in the Pleistocene layer of Port Island indicated by element 384 and 1539 in **Fig.11** are plotted in **Fig. 12.** In the fill soil, the effective stress path rapidly decreased and approached to the origin of the coordinate as shown at the bottom in **Fig.12**(a). In accordance with this, the axial strain difference was gradually induced as shown in the upper row of the same figure, The magnitude of the shear strain γ_{xy} in the upper fill was relatively small.

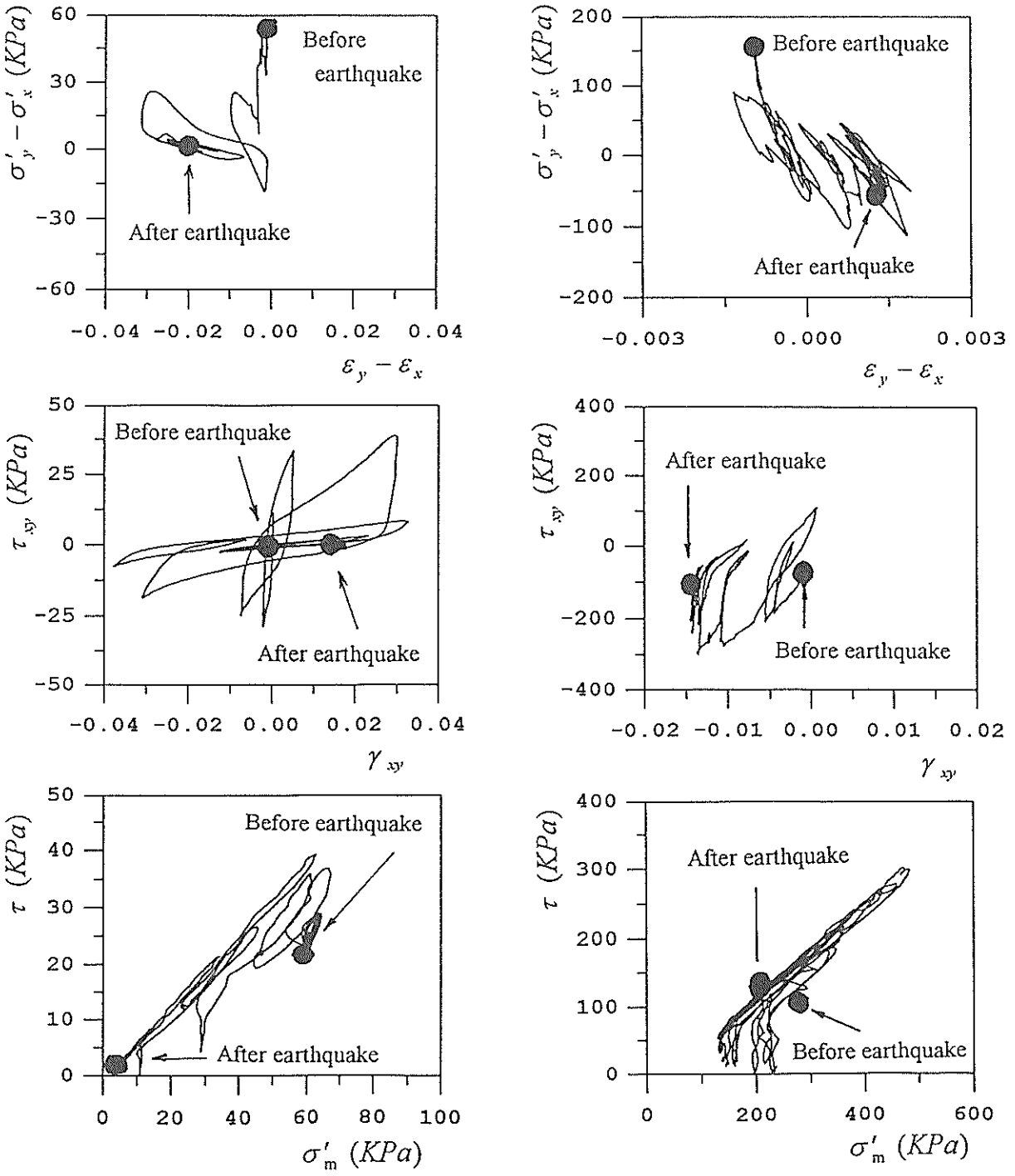

(a) In the upper fill soil (b) In the Pleistocene layer of Port Island

Fig. 12 Predicted stress strain relation and stress path

It can also be seen from **Fig.12**(b) that, in the element 1539 of Pleistocene layer of Port Island, the effective stress path gradually approached the failure line with fluctuation around the initial deviatoric stress. Even the effective mean stress was once decreased 35 percent, the final value, however, was back to 220KPa. In accordance with this,

the axial strain difference was gradually induced as shown in the upper row of the same figure. The shear strain γ_{xy} was also gradually induced but remained at a relatively small level. All this results indicate that the deformation of pneumatic caisson foundation was likely to be induced due to the existence of initial stress and its release in accordance with overall softening of saturated soil based on the mechanism of cyclic mobility.

5. INFLUENCE OF EXCESS PORE WATER PRESSURE

In order to evaluate the effect of the excess pore water pressure increase in the foundation, the following three cases of analyses were performed by introducing an artificial soil model, to be called non-liquefiable soil model which has the same properties as those used in the aforementioned analysis but completely lacks the characteristics of dilatancy. The case which dealt with the actual bridge foundation during the earthquake shown in the previous is designated as Case-1. Case-2 is to idealize both the upper fill and the Pleistocene layer being the non-liquefiable soils. Case-3 is to idealize only upper fill non-liquefiable, and Case-4 is to idealize only Pleistocene layer non-liquefiable.

In order to quantify the individual effect of excess pore water pressure increase in the upper fill and Pleistocene layer, the principal results of the deformation were summarized in **Table 4** including those of Case-1. The excess pore water pressure distribution for case-2 to 4 are shown in **Fig. 13.** The results of Case-2 shown that the seaward displacement is 0.31m at the top of a caisson while 0.17m at the top of the other caisson, resulting in a total of 0.48m. This is the displacement induced purely due to the inertia force of the earthquake. Consequently, the excess pore water pressure increase in the foundation soil was to increase the displacement about 2 times as those induced purely by the seismic inertia force.

Table 4 Computed horizontal displacement of foundation

Case	P2(m)	P3(m)	Total(m)
Case-1	0.46	0.48	0.94
Case-2	0.31	0.17	0.48
Case-3	0.28	0.34	0.62
Case-4	0.46	0.16	0.62

The results of Case-3 indicate that the excess pore water pressure increase in the upper fill soil and replaced sand will increase the deformation of caisson about 1.5 times of those induced in Case-2. It is speculated from the results that the soil improvement in the upper soil can reduced the displacement of caisson foundation about 35%. The excess pore water pressure increase in the Pleistocene layers under the caisson P3 for Case-4 is to increase the displacement about 50 percent of those induced in Case-2. It is also noted from **Fig.9** (a) that the shear deformation under caisson foundation P3 is much larger than that under caisson foundation P2. This may be due to the higher excess pore water pressure in the Pleistocene layer under the caisson P3.

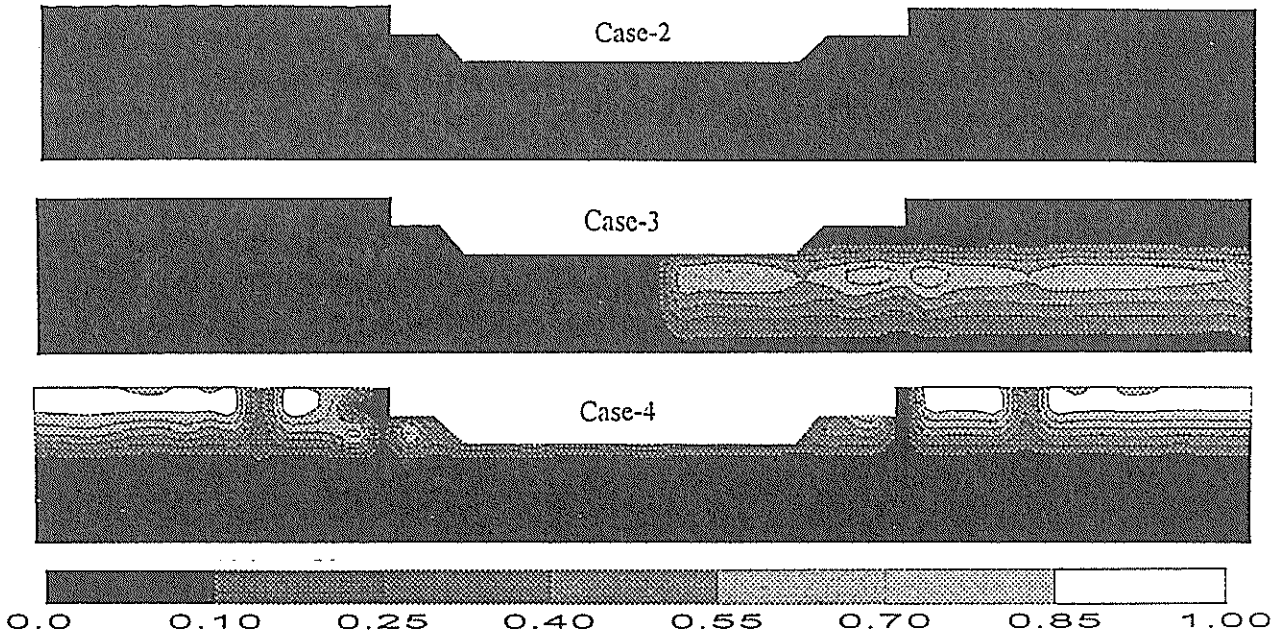

Fig. 13 Computed excess pore water pressure for Case-2 to 4

6. EFFECT OF SOIL IMPROVEMENT

The soil improvement was taken around the caisson by the Kobe city after earthquake as a remedial measure against liquefaction. The High Pressure Jet Grouting scheme and Gravel Pile scheme were used to improve the shear and liquefaction resistance of soil. The areas of improvement are shown in Fig.14[8].

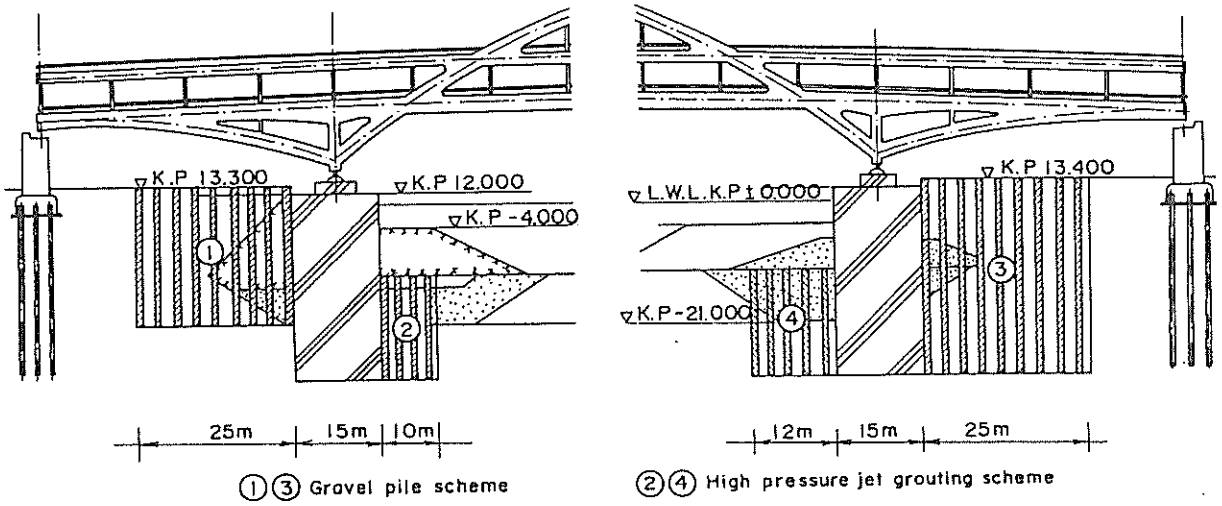

(a) In the Fourth Pier (b) In the Port Island

Fig. 14 Soil improvement area

In order to evaluate the effectiveness of these improvement, the analysis for the improved foundation was conducted here. The same cross section as shown in **Fig.1** was used and the same input motions as shown in **Fig. 7** are used for the post improvement analysis. The parameters used for the improved area was shown in **Table 5.** The computed residual displacement is shown in **Fig.15.** The computed horizontal residual displacement are 0.19m on the top of caisson in the Fourth Pier side and 0.39m in the Port Island side, resulting in a total of 0.58m seaward displacement. The displacement was reduced about 38 percent from the non-improvement case as shown in **Table 6.** The effectiveness of the improvement is comparable to Case-3, where the complete area of the upper fill layer is assumed. The distribution of excess pore water pressure ratio is shown in **Fig.16.** Comparing to **Fig. 11,** the excess pore water pressure around the caissons is restrained, and the range of liquefaction was obviously reduced. The soil improvement was, thus, confirmed effective.

Table 5 Parameters for improved foundation

Soil No.	γ (tf/m^3)	G_a (tf/m^2)	K_{ma} (tf/m^2)	σ'_{ma} (tf/m^2)	ϕ_f (deg.)
①	1.80	8800	23020	6.430	40
②	1.80	10600	27730	14.67	40
③	1.80	8800	23020	6.430	40
④	1.80	10600	27730	14.67	40

Table 6 The comparison of result with and without improvement

	Improvement	P2	P3
Horiz. disp. (m)	Without	0.46	0.48
	With	0.19	0.39
Vertical disp. (m)	Without	0.12	0.11
	With	0.04	0.04
Inclination (deg.)	Without	0.68	0.07
	With	0.28	0.07

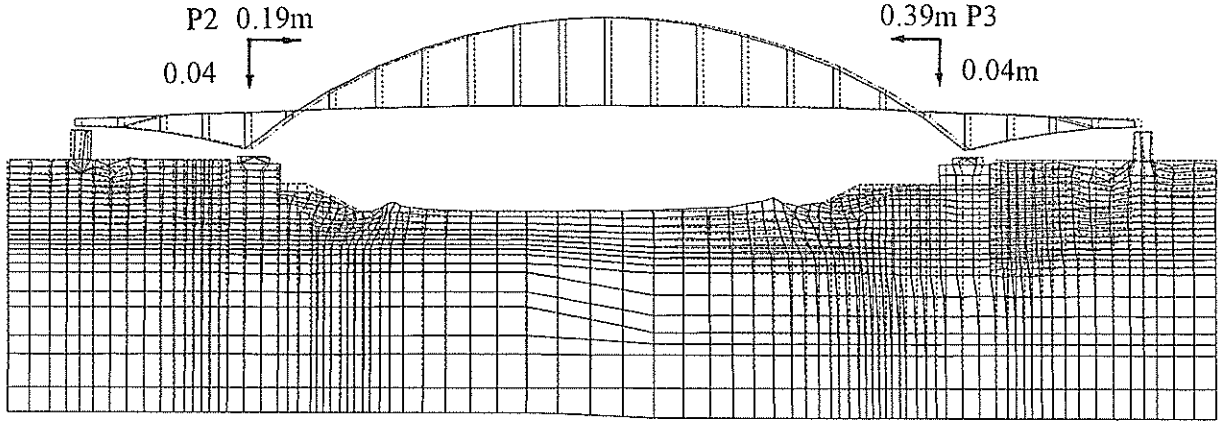

Fig. 15 Computed residual deformation with improvement

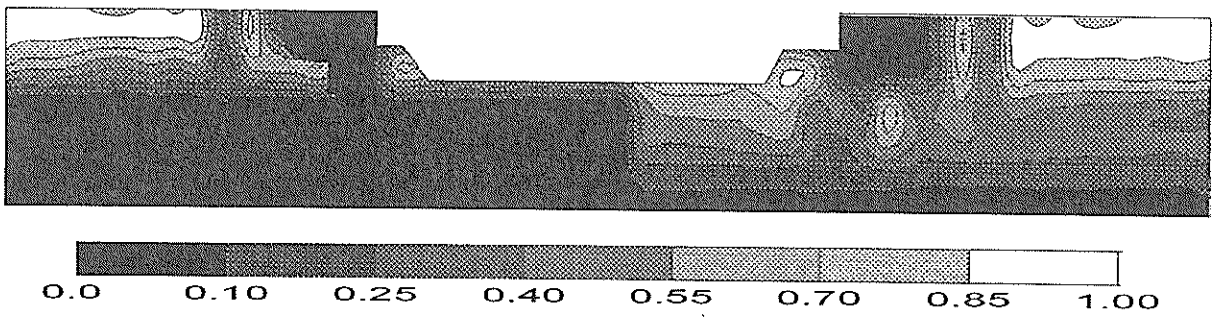

Fig. 16 Computed excess pore water pressures with improvement

7. CONCLUSIONS

Effective stress analysis was performed on the deformation of the pneumatic caisson foundations of the Kobe Ohashi Bridge at the 1995 Great Hanshin earthquake. These pneumatic caisson foundations were embedded to a firm foundation at a depth of about 30 m below the ground surface. It was a rigorous test for the effective stress model to simulate the deformation of soil-structure systems. Major conclusions derived from this analysis are as follows.

(1) The computed horizontal residual displacements were 0.46 m on a caisson at the Fourth Pier and 0.48 m on another caisson at the Port Island, resulting in a total of 0.94 m toward sea. This was consistent with the measured residual displacements ranging from 0.6 to 0.8 m at the Kobe Ohashi Bridge after the earthquake.

(2) This result indicates that the effective stress model used in this study has the potential ability to evaluate the deformation of pneumatic caisson foundations undergoing strong earthquake motion.

(3) The mechanism of deformation of the pneumatic caisson foundations as derived from this study is due to the existence of the deviator stresses in the foundation soil before the earthquake and the release of these deviator stresses in accordance with overall softening of saturated soil undergoing cyclic loading.

(4) A series of parametric studies indicate that the effect of the excess pore water pressure generation in the foundation soil is to increase the deformation about twice as large as that purely caused by the seismic inertia force. In particular, the soil improvement implemented after the earthquake was confirmed effective to reduce the deformation of the pneumatic caissons.

ACKNOWLEDGMENT

The supports of the STA Fellowship of Japan and the National Science Foundation of China are acknowledged.

(Received on March 31,1997)

REFERENCES

1) Iai, S., Matsunaga, Y. and Kameoka, T. 1992a, Strain space plasticity model for cyclic mobility, *Soils and Foundations*, Vol.32, No.2, pp.1-15

2) Iai, S., Matsunaga, Y. and Kameoka, T. 1992b, Analysis of cyclic behavior of anisotropically consolidated sand, *Soils and Foundations*, Vol.32, No.2, pp.16-20

3) Zienkiewicz, O.C. 1977, The Finite Element Method, 3rd edition, McGraw-Hill Book Co.

4) Inagaki, H., Iai, S., Sugano, T., Yamazaki, H., and Inatomi, T. 1996, Performance of caisson type quay walls at Kobe port, *Soils and Foundations, Special Issue.* pp.119-136

5) Ministry of Transport ed. 1993, Handbook for Liquefaction remediation of reclaimed land, pp.243-245(in Japanese)
6) Sugito, M., Sekiguchi, K., Yashima, A., Oka, F., Taguchi.Y and Kato, Y. 1996, Correction of orientation error of borehole strong motion array records obtained during the South Hyogo Earthquake of Jan.17, 1995, *Journal of Structural Mechanics and Earthquake Engineering*, JSCE, 12(3 and 4), pp.51-63
7) Zienkiewicz, O.C. and Bettess, P. 1982, Soils and other saturated media under transient, dynamic load conditions, *Soil Mechanics-Transient and Cyclic Loads*, Pande Zienkiewicz eds., John Wiley and Sons, pp.1-16
8) Okashita, K., Okutani S., Ojima S., and Fujita, C., Numerical study on seismic damage of caisson foundations due to ground liquefaction and examination of countermeasures. *Proc. of Civil Engineer Society of Japan on Great Hanshin-Awaji Earthquake*, Tokyo, pp.611-618(in Japanese)
9) Architectural Institute of Japan, 1988, Handbook of Structural design of architecture foundation, pp.163-169(in Japanese)
10) Yoshimi, Y., 1991, Liquefaction of Sandy Deposit, *Gihoudo Press*, 2nd edition, pp.86(in Japanese)

APPENDIX

Calibration of model parameters for dilatancy

The details for calibrating the model parameters for dilatancy were performed as follows. First, the empirical relation between the SPT N-values and liquefaction resistance[9], shown in **Fig. A1**, was used for specifying the level of resistance for 15 load cycles. The level of resistance was then used to represent liquefaction resistance curve, specified in terms of a relation between the shear stress ratio vs. load cycles. This was obtained based on the relation for correcting the effect of earthquake magnitude, shown in **Fig. A2**, and the relation between earthquake magnitude and equivalent number of load cycles[10]. Following these procedures, the liquefaction resistances of the soil deposits at Kobe Ohashi Bridge were estimated from the in-situ geotechnical data.

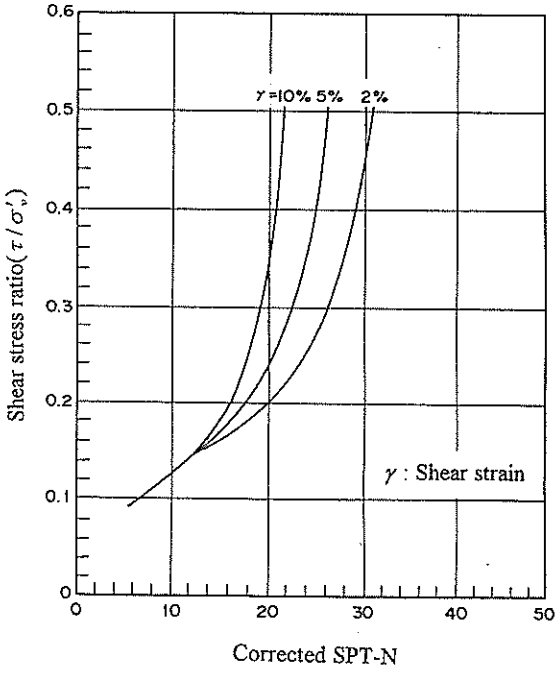

Fig. A1 The shear stress ratio vs corrected SPT-N value(After AIJ, 1988)

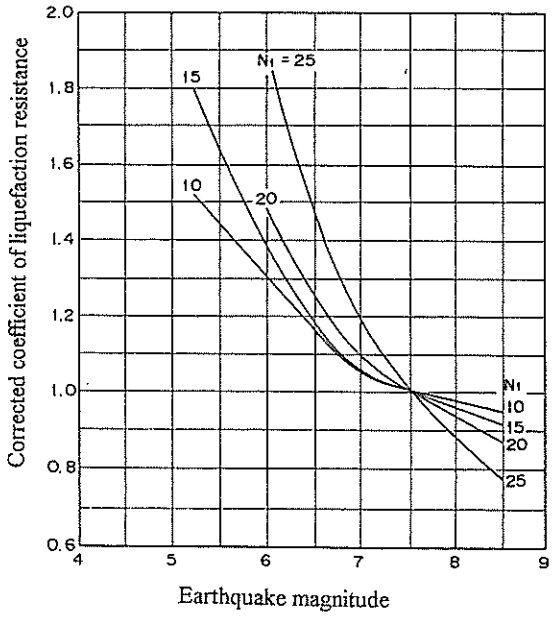

Fig. A2 The corrected coefficient for liquefaction resistance to SPT N values(After Yoshimi, 1991)

As shown in **Fig. A1**, the estimation of the liquefaction resistance is not easy for SPT N-values larger than about 25. For estimating the parameters for this case, an extrapolation was performed for the parameters from those given for smaller SPT N-values as shown in **Fig. A3** and **Table A1**. Based on these procedures, the parameters shown in **Table 4** was obtained.

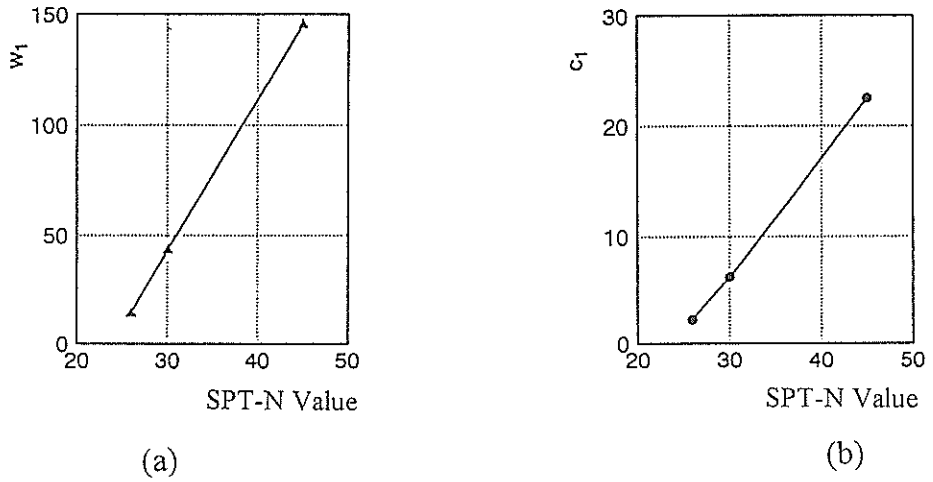

Fig. A3 Dilatancy parameters for (a) w_1 and (b)c_1

Table A1 The dilatancy parameters

SPT-N value	w_1	c_1	p_1	p_2	S_1
26	13.8	2.25	0.5	0.6	0.005
30	45.5	4.25	0.5	0.6	0.005
50	145.5	22.5	0.5	0.6	0.005